RSC Advances

PAPER

View Article Online
View Journal | View Issue

Cite this: *RSC Adv.*, 2016, **6**, 20202

Photo-immobilization of bone morphogenic protein 2 on PLGA/HA nanocomposites to enhance the osteogenesis of adipose-derived stem cells

Tianlin Gao,[ab] Weiwei Cui,[b] Zongliang Wang,*[a] Yu Wang,[a] Ya Liu,*[b] Ponnurengam Sivakumar Malliappan,[cd] Yoshihiro Ito[cd] and Peibiao Zhang*[a]

Received 28th December 2015
Accepted 9th February 2016

DOI: 10.1039/c5ra27914c

www.rsc.org/advances

Lack of bioactivity has seriously restricted the development of biodegradable implants in bone tissue engineering. In this study, Bone Morphogenic Protein 2 (BMP-2) was photo-immobilized on the poly(lactide-*co*-glycolide)/hydroxyapatite (PLGA/HA) and pure PLGA composites *via* photo-reactive gelatin (Az-Gel). The results demonstrate that the Az-Gel facilitates efficient and long-term immobilization of peptides on the surface of PLGA. The immobilization of Az-Gel enhanced the adhesion and proliferation of Mouse Adipose-Derived Stem Cells (ADSCs), while HA incorporation facilitated cellular osteodifferentiation. The immobilization of BMP-2 induced the osteogenesis of the ADSCs, indicated by alkaline phosphatase activity, quantitative real-time polymerase chain reaction (qRT-PCR) analysis and mineralization on the deposited substrates. Furthermore, the surface immobilization of BMP-2 could not only reduce the amount of growth factor, but also have a long-term osteoinductive effect. Therefore, it is considered that the surface modification method has a great potential for the enhancement of osteointegration of biodegradable bone implants.

Introduction

Bone tissue engineering has been developed as a promising therapy to treat bone defects because of the limitations of bone tissue regeneration potential and current treatments.[1,2] Biodegradable polymers have been widely used to prepare tissue engineering scaffolds due to their versatile properties.[3,4] Synthetic biodegradable polymers such as poly(lactic-*co*-glycolic acid) (PLGA) have been extensively studied for tissue engineering, alone or combined with other active factors, since the polymers possess good mechanical properties, low immunogenicity and toxicity, and an adjustable degradation rate.[5–7] Hydroxyapatite ($Ca_{10}(PO_4)_6(OH)_2$, HA) is an effective component for biomimetic materials because of its similarity with the mineral phase of natural bone.[8] It has the abilities of bone binding and osteoconductivity, and has also been widely used in bone tissue engineering.[9,10] Our group is committed to the study of the biodegradable porous PLGA/HA scaffolds for the bone repair, using the solvent casting/particulate leaching method.[11,12] However, the hydrophobicity of PLGA is unfavourable for osteocyte adhesion and HA alone possesses limited osteoinductive ability, which has restricted their regenerative stimulation of large bone defects.[13] One strategy to solve this problem is surface modification with incorporation of cell growth factors into the 3D scaffolds.[14,15]

Growth factors, such as bone morphogenetic proteins (BMPs), are often employed to induce osteogenic differentiation and promote bone regeneration. BMPs are osteoinductive growth factors that can induce bone formation both *in vivo* and *in vitro* and have been widely used in tissue engineering approaches for the repair of bone injuries and bone defects.[14,16] Among the BMP family, bone morphogenic protein-2 (BMP-2), a proven strong osteoinductive factor, stimulates the differentiation of osteoprogenitor cells into mature osteoblasts.[17,18] The BMPs can be delivered by direct injection and release from a carrier.[19–21] However, conventional biomaterial delivery vehicles commonly suffer from limitations that can result in low retention of growth factors at the site of interest, supra physiological levels or short duration.[22] Compared to these conventional administrations, the immobilization method has attracted much attention as a new delivery method.[23–26] It has been reported that immobilized growth factors can be more efficiently used than free growth factors with lower amount of growth factors required. Meanwhile, the immobilized growth factors can be localized and retained in the designated location to maintain the stimulation effect for a long period.[26,27] Gelatin, obtained by the denaturation of collagen, was selected as the

[a]*Key Laboratory of Polymer Ecomaterials, Changchun Institute of Applied Chemistry, Chinese Academy of Sciences, Changchun, 130022, China. E-mail: zhangpb@ciac.ac.cn; wangzl@ciac.ac.cn*

[b]*School of Public Health, Jilin University, Changchun, 130021, P. R. China. E-mail: liuya@jlu.edu.cn*

[c]*Nano Medical Engineering Laboratory, RIKEN, 2-1-Hirosawa, Wako, Saitama 351-0198, Japan*

[d]*Emergent Bioengineering Materials Research Team, RIKEN Center for Emergent Materials Science, 2-1-Hirosawa, Wako, Saitama 351-0198, Japan*

biological polymer for incorporation due to its low immunogenicity, biodegradability, and biocompatibility.[28,29] A photo-reactive gelatin (Az-Gel), which could be immobilized on various matrices by UV-irradiated, was synthesized by our group to either improve the matrices biocompatibility or immobilized bio-signal molecules onto them.[30] Using photo-reactive gelatin to immobilize BMP-2 on the surface of PLGA/HA composites may not only improve the hydrophilicity of the composites, but also perform long term osteoinductive activity together with HA.

In this study, BMP-2 was photo-immobilized onto the surface of PLGA/HA composites *via* Az-Gel. As shown in Scheme 1, BMP-2 was first mixed with Az-Gel solution. Then the mixture was immobilized on the surface of the PLGA/HA composites *via* UV irradiation. The improvement of hydrophilicity and mouse Adipose-Derived Stem Cells (ADSCs) adhesion were investigated to evaluate the effect of surface-immobilized gelatin. Afterwards, the effect of osteogenic differentiation of ADSCs was investigated about the combined effect of immobilized BMP-2 and HA.

Experimental section

Materials

PLGA (lactide/glycolide ratio = 80/20, M_n = 85 000) was synthesized by Changchun Institute of Applied Chemistry, Chinese Academy of Sciences (CIAC, China). Dichloromethane (DCM) and *N*,*N*-dimethylformamide (DMF) were obtained from Beijing Chemical Works. Cetylpyridinium chloride (CPC) was purchased from Aladdin Chemistry Co. Ltd. Recombinant human BMP-2 was purchased from UB Biotech.

PLGA/HA films preparation

As the main purpose of this study is to improve the surface bioactivity of biodegradable PLGA and PLGA/HA composites, we prepared PLGA and PLGA/HA films, instead of scaffolds, to better observe the surface properties of these biodegradable scaffolds made of these materials. Briefly, 24 × 24 mm siliconized cover slides were prepared by treatment with 2% dimethylchlorosilane (DMDC, Fluka) and baking at 180 °C for 4 h. 10 mg HA were dispersed into 1 mL DCM and 90 mg PLGA were dissolved in 9 mL DCM. Then the HA solution was dropped into PLGA solution with stirring of 500 rpm for 24 h. The total solids content of HA was 10% (w/w). A total of 50 μL of the solution was transferred to a cover slide to form a thin film by evaporation in the air for 30 min and in a vacuum dryer for 48 h at the room temperature. Pure PLGA films were also prepared at the same conditions.

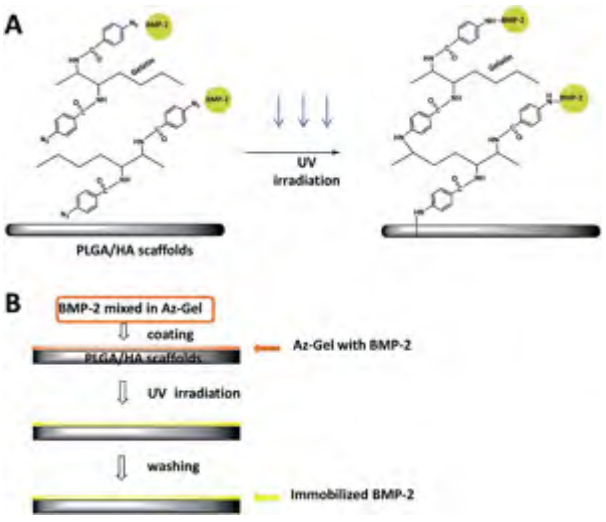

Scheme 1 Schematic illustration of Az-Gel-assisted immobilization of BMP-2 on PLGA/HA scaffolds for enhancing proliferation and osteogenic differentiation of ADSCs.

Surface immobilization of BMP-2

The photo-reactive gelatin, referred to Az-Gel, was fabricated by our coworker.[26] Briefly, gelatin was dissolved in 10 mL of water and added to 20 mL of a DMF solution containing 25.8 mg *N*-(4-azidobenzoyloxy)succinimide while being stirred on ice. After a stirred incubation at room temperature for 24 h, the solution was ultrafiltrated using a Millipore (Billerica, MA, USA) ultrafiltration membrane (molecular weight: 10 000). The dialyzed sample was freeze-dried for photo-immobilization.

The photo-immobilization of BMP-2 was performed as followed. Az-Gel (100 μg) and various concentrations of BMP-2 were mixed in distilled water (100 μL), so that the final concentrations of BMP-2 in the solution were 1, 10 and 100 ng mL^{-1}. Then the aqueous solution was cast on the films and air-dried at room temperature. The films were then UV-irradiated using a UV lamp (CL-1000 Ultraviolet Crosslinker, USA) from a distance of 5 cm for 20 s (16 mW cm^{-2}). Afterwards, the composites were washed repeatedly with distilled water to remove the unfixed molecules and used for analysis and cell culture without further treatment (Az-Gel@PLGA/BMP-2 and Az-Gel@PLGA/HA/BMP-2). Pure Az-Gel was also immobilized on the surface of PLGA and PLGA/HA films at the same conditions just without BMP-2 incorporation (Az-Gel@PLGA and Az-Gel@PLGA/HA).

Surface characterization

Fourier transform infrared spectroscopy (FTIR, Perkin Elmer, FTIR-2000) was used to determine the chemical structure of the films before and after photo-immobilization.

Static air–water contact angle measurements of the films were obtained using the sessile drop method on a contact angle system (VCA 2000, AST).

Culture of ADSCs

ADSCs were isolated from adipose tissues obtained from BALB/c mouse (SCXX (JING) 2009-0015) using an established protocol as before.[13] The animals were provided by Jilin University, Changchun, China and treated according to the NIH guide for the care and use of laboratory animals. Briefly, the tissues were extracted and washed with phosphate buffer saline (PBS) on a separating sieve, then treated with 0.075% collagenase type I (Gibco) for 1 h at 37 °C under shaking. Cells were collected by centrifugation at 1200 rpm, 4 °C for 10 min and cultured in

tissue culture flasks with Dulbecco's Modified Eagle Medium (DMEM, Gibco) supplemented with 10% fetal bovine serum (Gibco), 100 U mL^{-1} penicillin and 100 U mL^{-1} streptomycin (Sigma). After the cells were attached, the medium was removed, washed with PBS, and replaced with fresh medium. The cells were passaged for cell expansion when cultured to 80% confluency. ADSCs of passages 2 or 3 were used for the experiments in this study.

Cell adhesion and proliferation

ADSCs were seeded onto various films at an initial seeding density of 2×10^4 cells per cm^2 and incubated for 3, 6, and 12 h, respectively. The cells were washed three times with PBS, fixed with 4% paraformaldehyde (PFA) at room temperature in PBS for 10 min, dyed with 2% fluoresceinisothiocyanate (FITC) DMSO/H_2O solution for 10 min, and then washed with PBS for three times. Cell attachment was observed qualitatively under a reverse microscope (TE2000U, Nikon, JPN). The fluorescence pictures were taken by Digital Camera (DXM1200F, Nikon) and analyzed with "NIH ImageJ" software.

To investigate the effect of surface-modification on the cell adhesion and spreading, the organization of actin filaments of adherent cells cultured on various films was evaluated after 24 h with or without surface-modification. ADSCs were cultured on films at a density of 2×10^4 cells per cm^2. Cytoskeletons were identified following double stain of actin staining (red) using Alexa Fluor 488 phalloidin and nuclei staining (blue) using 4,6-diamidino-2-phenylindole dihydrochloride (DAPI, Invitrogen). ADSCs fixed using 4% PFA for 15 min, followed by washing in PBS for three times. Cell membranes were permeabilized in 0.1% Triton X-100 for 10 min and blocked in 1% BSA solution for 30 min, followed by washing in PBS for three times respectively. Afterwards, cells were incubated with phalloidin for 15 min and DAPI for 3 min and then washed in PBS three times. Samples were observed and imaged using confocal laser scanning microscope (CLSM, Zeiss LSM 780).

Cell proliferation on different films was determined as followed. The films were sterilized by immersing in 70% alcohol for 30 min. After washed by PBS for three times and immersed in cell culture medium overnight, they were placed into 24-well plate to cover the bottom of wells. 1 mL ADSCs suspension (2×10^4 cells per mL) was then seeded into each well. The plates were incubated at 37 °C in a humidified 5% CO_2 atmosphere and the culture medium was replaced every two days. After 1 d, 4 d and 7 d culture, the medium was replaced by Cell Counting Kit-8 (CCK-8, Dojindo, Japan). The absorbance values at 450 and 600 nm were measured after 2 h of incubation on a multifunctional microplate scanner (Tecan Infinite M200).

Alkaline phosphatase activity

ALP activities of ADSCs cultured for 7 d and 14 d were evaluated by measuring the amount of *p*-nitrophenol produced using *p*-nitrophenol phosphate substrate (*p*NPP) solution (Sigma). Briefly, the medium of each well was carefully removed at the end of the incubation. Then ADSCs were washed three times with PBS and lysed in RIPA buffer before freezing at −80 °C for 30 min and thawing at 37 °C. Afterwards, 50 μL ALP substrate for each well was added. The absorbance at 405 nm was read by multifunction microplate scanner after incubated in the dark at 37 °C for 30 min. The average OD values were used to reflect the level of ALP activities correspondingly.

Quantitative real-time polymerase chain reaction

ADSCs cultured on various films were incubated at 7 d and 14 d. Then, the mRNA expression of osteogenesis-related genes was quantitatively assessed using qRT-PCR technique.[31] The total RNA was extracted using TRIzol reagent (Invitrogen) according to the manufacturer's protocol. The concentration and purity of RNA were estimated using nanodrop plates (Tecan Infinite M200) and reverse transcribed as described in M-MLV manual (Promega). The expression of osteogenic markers was quantified by qPCR SYBRGreen Mix Kit (TaKaRa). Gene-specific primers including glyceraldehyde-3-phosphate dehydrogenase (GAPDH), anti-runt-related transcription factor 2 (RUNX2), osteopontin (OPN) and osteocalcin (OCN) were designed using the primer design software of beacon 5.0 (Table 1). qRT-PCR was conducted by StepOnePlus real-time PCR system (Applied Biosystems, CA) and expression levels were obtained using threshold cycles (C_t) which were determined by the iCycleriQ Detection System software. Relative transcript quantities were calculated using the $\Delta\Delta C_t$ method. The gene GAPDH was used as a reference gene and was amplified along with the target genes from the same cDNA samples. The difference in C_t of the sample mRNA relative to GAPDH mRNA was defined as the ΔC_t. The difference between the ΔC_t of the control cells and the ΔC_t of the cells grown on the treated films was defined as the $\Delta\Delta C_t$. The fold change in mRNA expression was expressed as $2^{-\Delta\Delta C_t}$.

Mineralization

After 20 d of culture, calcium deposition by ADSCs was analyzed by Alizarin Red S staining. The cells were fixed in 4% paraformaldehyde in PBS for 15 min at room temperature and then washed with acidic PBS (pH 4.2) for three times. The cells were then incubated in 2% (w/v) Alizarin Red S (Sigma) solution at 37 °C for 20 min. The solution was freshly prepared before use by dissolving Alizarin Red S in distilled water. After the removal of Alizarin Red S solution, the stained cells were rinsed with acidic PBS three times and observed under a light microscope. Calcium quantification was measured *via* CPC treatment.[32] ARS-stained membrane films were washed with distilled water and treated with 1 mL of 10% CPC solution for 1 h to desorb the calcium ions. Absorbance of the solution was read at 540 nm in multifunctional microplate scanner and normalized to the cell number from the CCK-8 assay (OD_{540}/OD_{450}).

Statistical analysis

The data presented are the mean (standard deviation ± SD). Independent and replicated experiments were used to analyze the statistical variability of the data using one-way analysis of variance, with $p < 0.05$ being statistically significant ($^*P < 0.05$).

Table 1 Sequences of primers for the qRT-PCR

Gene	Forward primer sequence	Reverse primer sequence
RUNX 2	5-GCCCTCATCCTTCACTCCAAG-3′	5-GGTCAGTCAGTGCCTTTCCTC-3′
OPN	5-TCAGGACAACAACGGAAAGGG-3′	5-GGAACTTGCTTGACTATCGATCAC-3′
OCN	5-CCTCACACTCCTCGCCCTATT-3′	5-CCCTCCTGCTTGGACACAAA-3′
GAPDH	5-CAACCTGGTCCTCAGTGTAGC-3′	5-CGTGCCGCCTGGAGAAACCTGCC-3′

Results and discussion

Characterization of films

The FT-IR spectra of the films were performed to help determine the Az-Gel immobilization. Fig. 1 showed the broad absorption band of Az-Gel@PLGA at 3000–3600 cm^{-1}, which were assigned to the vibrations of –OH and $–NH_2$. And another broad absorption band at 1550–1660 cm^{-1} represented $–NH_2$. As there were no $–NH_2$ in the molecules of PLGA, the absorption band of $–NH_2$ indicated that the Az-Gel was immobilized on the surface of PLGA films. The spectra of PLGA/HA films showed similar changes after Az-Gel immobilization. All of the variations of the FT-IR spectra conformed that Az-Gel was successfully immobilized on the surface of both the PLGA and PLGA/HA films.

We measured the water contact angle of these films surfaces to analyze the change in wetting of the polymer surface. Pure PLGA surfaces exhibited water contact angles of 82.48 ± 8.52° (Fig. 2a), and PLGA/HA surfaces exhibited 78.69 ± 1.72° (Fig. 2b) due to the exposure of HA on the surface. Az-Gel immobilization decreased the contact angle of PLGA and PLGA/HA surfaces (67.32 ± 2.39° for Az-Gel@PLGA and 58.34 ± 1.83 for Az-Gel@PLGA/HA, Fig. 2c and d), indicating that the PLGA and PLGA/HA surfaces become more hydrophilic as a result of Az-Gel immobilization. This result suggested that the Az-Gel was immobilized on the surfaces of these films and could change the surface properties of these polymer substrates.

Cell adhesion and proliferation

The ADSCs proliferation was monitored quantitatively *via* the CCK-8 assay to measure the metabolic activity of the total population of cells for 1 d, 4 d and 7 d (Fig. 3A–C). The cells, seeded on the untreated PLGA film, showed the lowest levels of OD values of cell viability at each time points. Compared to PLGA film, the cell proliferation on the PLGA/HA film was promoted by the incorporation of HA. Our previous study has demonstrated that 10% HA could promote the adhesion on the PLGA films, due to its rough surface after HA doping.[33] The surface-immobilization of Az-Gel, at concentrations as low as 0.01 mg mL^{-1}, markedly increased the bioactivity of both PLGA and PLGA/HA films. Our previous work reported that upon UV irradiation, azidophenyl groups were photolyzed to generate highly reactive nitrenes that spontaneously formed covalent bonds with neighboring hydrocarbons on polymer surface.[34] This study had also demonstrated that the Az-Gel had covalent bond with PLGA hydrocarbons after UV irradiation and effectively improved the bioactivity of PLGA composites.

Despite of improving the cell adhesion and proliferation of the composites, Az-Gel was applied in the immobilization of

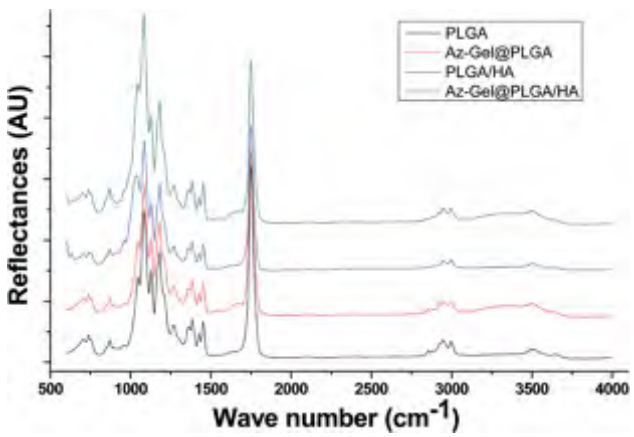

Fig. 1 FT-IR spectra of PLGA (black), Az-Gel@PLGA (red), PLGA/HA (blue) and Az-Gel@PLGA/HA (green) composites.

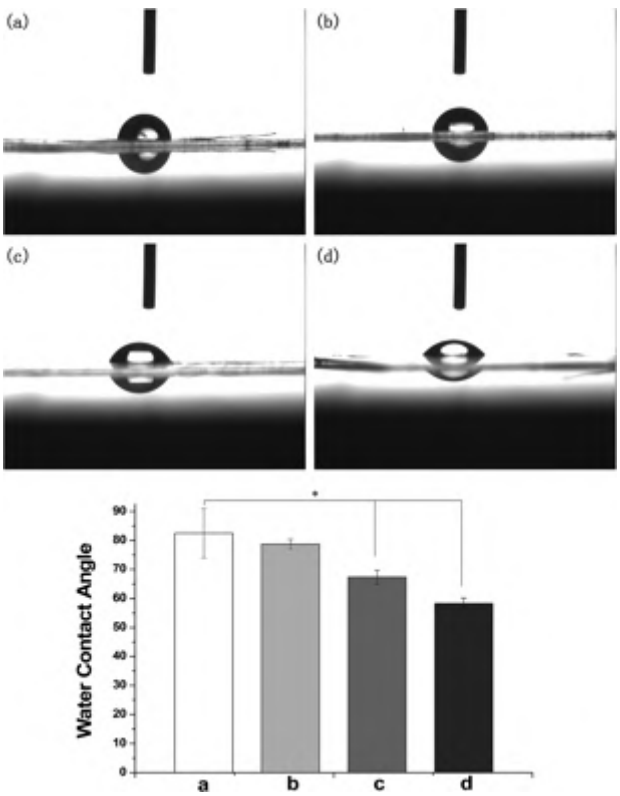

Fig. 2 Contact angle measurement of hydrophilic properties of PLGA (a), PLGA/HA (b), Az-Gel@PLGA (c) and Az-Gel@PLGA/HA (d). $P < 0.05$, $n = 4$.

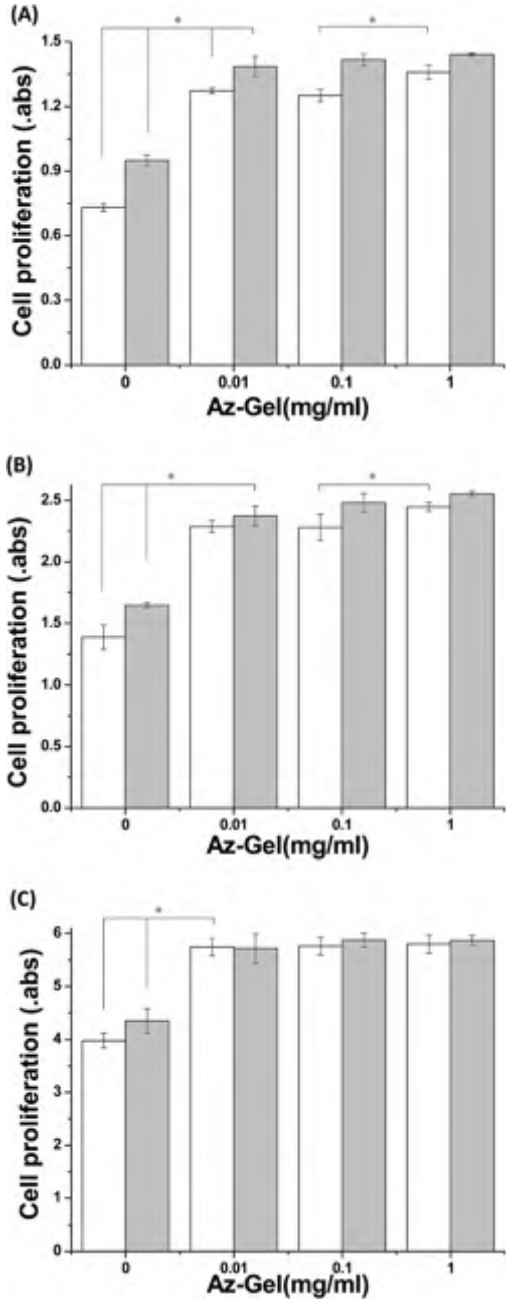

Fig. 3 CCK-8 test of ADSCs proliferation on PLGA (white) and PLGA/HA (light gray) films for 1 d (A), 4 d (B) and 7 d (C) after surface modification with Az-Gel of 0, 0.01, 0.1 and 1 mg mL^{-1}. $P < 0.05$, $n = 4$.

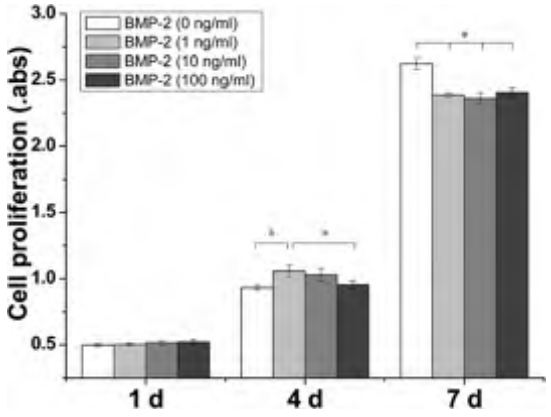

Fig. 4 CCK-8 test of ADSCs proliferation on different films immobilized with BMP-2 for 1 d, 4 d and 7 d. The concentrations of BMP-2 in the immobilized solution were 0, 1, 10 and 100 ng mL^{-1}. $P < 0.05$, $n = 4$.

BMP-2 to make the composites become more osteoinductive. It is found that the immobilization of BMP-2 *via* Az-Gel had little effect on the adhesion and proliferation of ADSCs compared to pure Az-Gel modification after 24 h culture (Fig. 4). After 4 d culture, higher OD value was found on the BMP-2 immobilized film with low concentration. However, with the increase of BMP-2 concentration, the OD value decreased, indicating BMP-2 with low concentration might promote the proliferation of ADSCs. After 7 d culture, the OD values of ADSCs on all the BMP-2 immobilized films were observed lower than the pure Az-Gel modified one. As the cell differentiation from stem cells to osteoblasts has gone through three main periods, cell proliferation, extracellular matrix (ECM) maturation and ECM mineralization. When the stem cells proliferated to a certain number, they suppressed their proliferation and started to differentiate to pre-osteoblasts.[35] We speculated that the lower OD values of ADSCs on all the BMP-2 immobilized films indicated the osteogenic differentiation from ADSCs to osteoblasts.

To more visually investigate the effect of the surface-modification for cell adhesion, half of the film was covered without UV irradiation and ADSCs were cultured on the film after repeat washing. As shown in Fig. 5, obvious cell adhesion and proliferation were observed on the surface-modified part after UV irradiation compared to the one without UV irradiation, which indicated the Az-Gel was efficiently immobilized on the surface of the PLGA after UV irradiation.

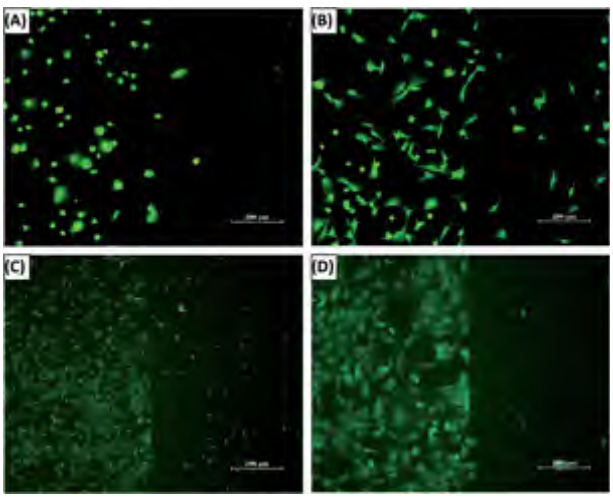

Fig. 5 Micrographs of ADSCs adhesion on the Az-Gel modified film at different times: 3 h (A), 6 h (B), 24 h (C and D). Left half of the film was irradiated by UV after the Az-Gel air-dried, while the right half was not irradiated. The scale bars of (A), (B) and (D) were 200 μm, while (C) was 500 μm.

ADSCs behavior on various films was also investigated. The cells were seeded on the various films in 24-well plate at a density of 2×10^4 cells per cm^2 and cultured for 3, 6, and 12 h, to further observe the adhesion and morphology of ADSCs. Most of cells were observed spread on the Az-Gel modified films (Az-Gel@PLGA and Az-Gel@PLGA/HA), while a few of the cells were observed on the non-modified films (PLGA and PLGA/HA) after 3 h culture. Afterwards, cells were observed spread on the Az-Gel modified films and appeared more similar to their natural morphology at 6 h (Fig. 6). The cells showed fully extended on all the films, but more extended cells were observed on the Az-Gel modified films after 12 h culture. The results of cytoskeleton and nuclear staining after 24 h culture showed that there were more cell quantities and positive cellular interaction with the supporting structure for Az-Gel modified films and exhibited better cytoskeleton, indicating that the surface modification is beneficial for cell growth and cell–cell communication. It is further supported the role of Az-Gel modification in promoting the attachment and proliferation of ADSCs. Meanwhile, it was also found that the immobilization of BMP-2 performed little effect on the adhesion of ADSCs, which was consistent with results of ADSCs proliferation. More interestingly, most cells on the non-modified films were in the forms of cell clumps, as compared to being evenly spread on the modified ones. We speculated the hydrophobicity of PLGA influenced the adhesion of the cells.

Alkaline phosphatase activity

ALP enzyme activity, which peaked during the pre-osteoblast stage of differentiation,[31] was chosen to explore the osteoinductive activity of the surface-modified films. Fig. 7 showed the ALP enzyme activities of ADSCs on the surfaces of different composites at 7 d and 14 d. A great increase in ALP activity of ADSCs was found on the BMP-2 modified films, higher than those of cells on the pure and the Az-Gel modified films, indicating that the cell differentiation toward osteogenesis was better on the BMP-2 modified films than other films. Immobilized of as low as 1 ng mL^{-1} BMP-2 significantly increased the ALP activity and the OD value of ALP activity was higher with the increase of BMP-2 concentration. The OD value of ALP activity on the Az-Gel@PLGA/BMP-2 (10 ng mL^{-1}, Fig. 7d) film was about 1.31 times and 1.27 times as that on the PLGA at 7 d and 14 d respectively. The doping of HA (Fig. 7e) could also increase the OD value of ALP activity and the OD value of ALP activity on the PLGA/HA film was 1.13 times and 1.11 times as that on the PLGA at 7 d and 14 d respectively, which was lower than that on

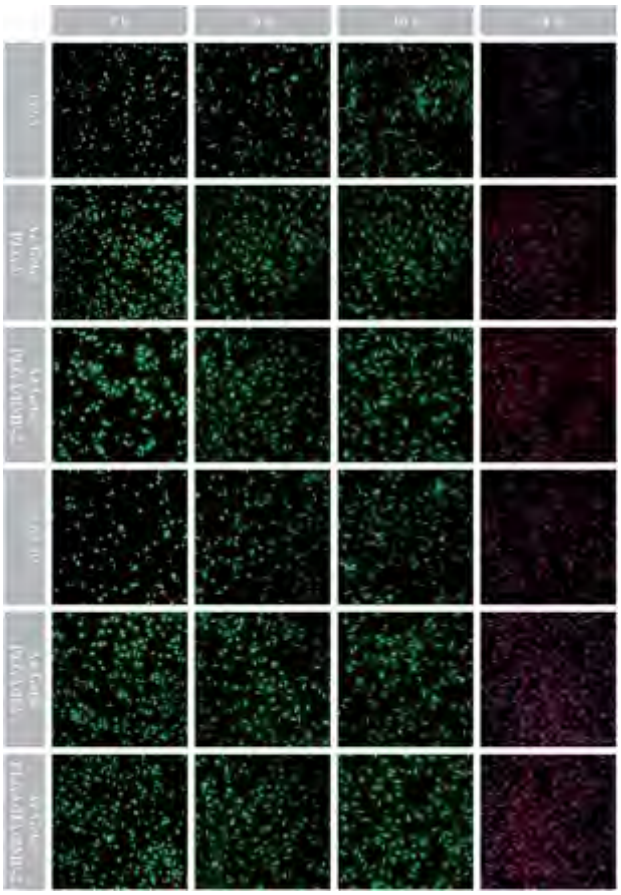

Fig. 6 CLSM micrographs showed FITC (green), actin microfilaments (phalloidintetramethylrhodamine B isothiocyanate, red) and nucleus (DAPI, blue) staining of ADSCs on different films for different times. All scale bar lengths are 20 μm.

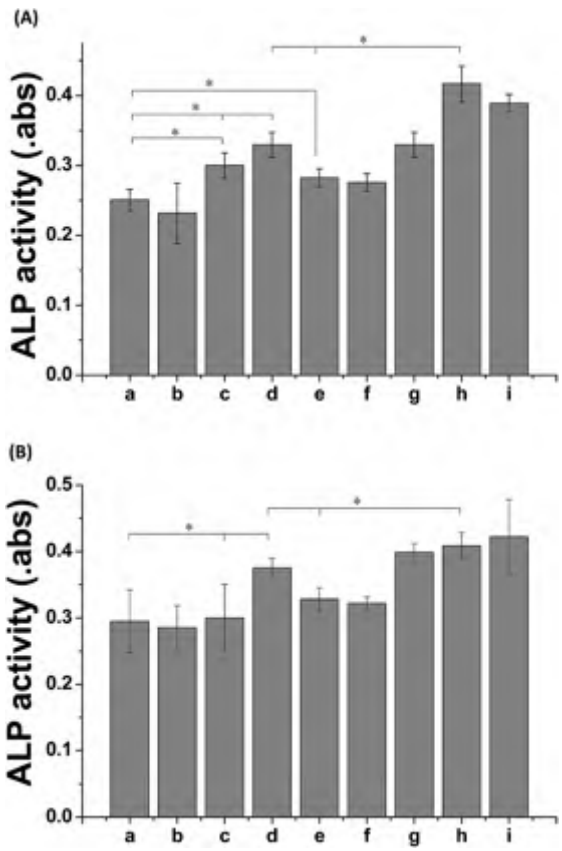

Fig. 7 ALP activities of ADSCs on different composites for 7 d (A) and 14 d (B) analyzed with *p*NPP kit: PLGA (a); Az-Gel@PLGA (b); soluble BMP-2 (10 ng mL^{-1}) (c), Az-Gel@PLGA/BMP-2 (10 ng mL^{-1}) (d); PLGA/HA (e); Az-Gel@PLGA/HA (f) and Az-Gel@PLGA/HA/BMP-2 (1, 10 and 100 ng mL^{-1}) (g–i). $P < 0.05$, $n = 4$.

Az-Gel@PLGA/BMP-2 film. It was reported that sustained exposure of W-20-17 cells to BMP-2 significantly increased ALP activity.[36] Meanwhile, our previous work found that HA could induce the osteogenic differentiation of ADSCs.[13] In this study, when BMP-2 was associated with HA (Az-Gel@PLGA/HA/BMP-2) (10 ng mL^{-1}, Fig. 7h), the composites exhibited stronger ability to promote ADSCs osteogenic differentiation than either PLGA/HA or Az-Gel@PLGA/BMP-2 (10 ng mL^{-1}, Fig. 7d) alone. We speculated that the combination of BMP-2 and HA had a synergistic effect in terms of osteogenic induction. As shown in Fig. 7, the OD values of ALP activity on the Az-Gel@PLGA and Az-Gel@PLGA/HA films did not exhibit significant difference with PLGA and PLGA/HA respectively. It is speculated that Az-Gel could just promote the ADSCs adhesion and proliferation, but not induce the osteogenic differentiation of ADSCs.

To better investigate the osteoinductive effect of immobilized BMP-2, BMP-2 was also directly added into the culture medium for comparison. The ALP activity of ADSCs increased in the well with soluble BMP-2 (10 ng mL^{-1}, Fig. 7c) after 7 d culture, but it decreased after 14 d culture. We speculated that BMP-2 might decrease with medium changing to that the soluble BMP-2 couldn't perform long-term effect. However, the immobilized BMP-2 could perform similar osteoconductivity as soluble BMP-2. Furthermore, the immobilized BMP-2 could retain the bioactivity for longer time than the soluble one. It was reported that immobilized growth factors could act in non-diffusion mode. These factors could bind to the cells receptors and exhibit long-term activity without down-regulation.[37] In this study, the immobilized BMP-2 bond to ADSCs receptors and induce the osteogenic differentiation of ADSCs for a long term. Meanwhile, comparing the total amounts of surface-immobilized BMP-2 *versus* BMP-2 solubilized within the well, the former (0.5 ng per well) was smaller than the latter (10 ng per well). Above all the surface-immobilized BMP-2 was more effective compared to solubilized BMP-2, and the former could perform long-term osteoconductivity compared to the latter.

Mineralization

The capacity of minerals deposition is a marker for mature osteoblasts, which can be used to conform that ADSCs differentiate to osteoblasts and enter into the mineralization phase to deposit mineralize ECM.[38] Osteogenic differentiation of ADSCs was induced on the different engineered films. After 20 days culture, the cells were stained with Alizarin Red S, which can bind to Ca^{2+} in mineralized ECM showing bright red stains, to examine calcium precipitation and mineralization. Fig. 8 is the optical microscopic images of ARS-stained films, confirming the variations in stain intensity for different films. The Alizarin Red stain showed slight reddish dots on both PLGA/HA and Az-Gel@PLGA/HA films but almost no positive stains were found over pure PLGA and Az-Gel@PLGA films, indicated that HA, not Az-Gel, could induce the osteogenic differentiation of ADSCs. Enhanced staining was observed over Az-Gel@PLGA/BMP-2 films, suggested that the immobilized BMP-2 also possess osteoinductive ability which is stronger than HA. In accordance with the ALP results, the most intense red staining was observed

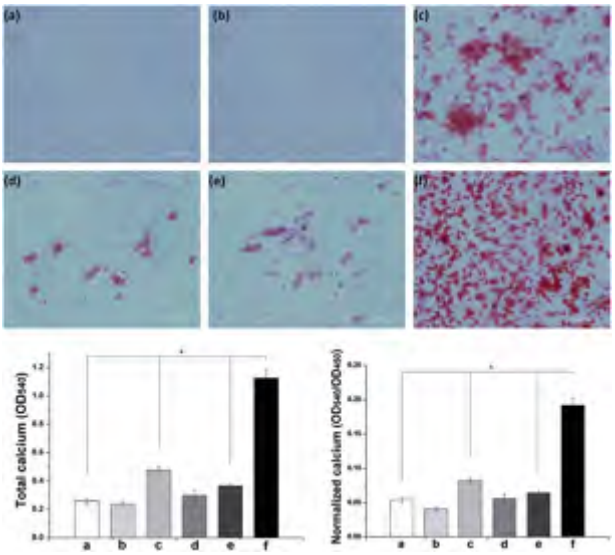

Fig. 8 Alizarin Red staining of ADSCs cultured on PLGA (a), Az-Gel@PLGA (b), Az-Gel@PLGA/BMP-2 (10 ng mL^{-1}) (c), PLGA/HA (d), Az-Gel@PLGA/HA (e) and Az-Gel@PLGA/HA/BMP-2 (10 ng mL^{-1}) (f) films at 20 d. All scale bar lengths are 200 μm. $P < 0.05$, $n = 4$.

over Az-Gel@PLGA/HA/BMP-2 films, which further conformed the additive effect of promoting osteogenic differentiation of ADSCs.

Quantitative cell mineralization was done after extracting ARS with 10% CPC to evaluate calcium-rich mineral deposits by ADSCs. Calcium quantification was recorded as total calcium content followed by normalized quantitative data with respect to cell number. After 20 days culture, the total calcium content in deposited minerals on PLHA/HA, Az-Gel@ PLGA/HA and Az-Gel@PLGA/BMP-2 films were significantly higher than that of PLGA films. And the highest calcium content in deposited minerals was still observed over the Az-Gel@PLGA/HA/BMP-2 films. The quantitative assessment of mineral deposition also depicted the same trends observed from ALP activity (Fig. 8), pointing out the importance of additive effect in the mineralization process of ADSCs by combination of HA and BMP-2.

Quantitative real-time polymerase chain reaction

The three main characteristics of cell differentiation from stem cells to osteoblasts are cell proliferation, ECM maturation and ECM mineralization. They are accompanied by certain up-regulation or down-regulation of genes in each stage. Fig. 9 showed the relative gene expression levels of various early, middle and later osteogenic marker genes to support the results from the ALP activity and calcium deposition. The selected mRNA expressions corresponds to specific genes were RUNX2, OPN and OCN. RUNX2 is an early differentiation marker observed at the early stage of differentiation, OPN expression is observed at the middle/late stage and OCN is at the late stage of differentiation.[32,35,39] In Fig. 8, up-regulation of RUNX2, OPN and OCN gene expression was found in PLGA/HA films, conforming the osteoinductivity of HA (Fig. 9c). After BMP-2 immobilization, much higher levels of these three gene

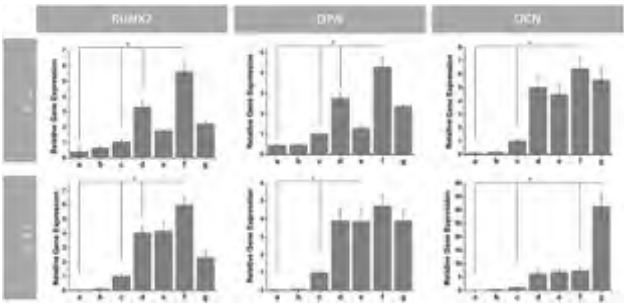

Fig. 9 Quantitative real-time PCR analysis of osteogenesis-related gene expression of RUNX2, OPN and OCN after ADSCs cultured for 7 d and 14 d: PLGA (a); Az-Gel@PLGA (b); Az-Gel@PLGA/HA (c); Az-Gel@PLGA/BMP-2 (10 ng mL^{-1}) (d); Az-Gel@PLGA/HA/BMP-2 (1, 10 and 100 ng mL^{-1}) (e–g). $P < 0.05$, $n = 4$.

expression were observed, indicating much stronger osteogenic induction by BMP-2 (Fig. 9d). A significant increase in the expression of the three genes was observed on the Az-Gel@PLGA/HA/BMP-2 (Fig. 9f), respectively, compared to cells on Az-Gel@PLGA/HA (Fig. 9c) and Az-Gel@PLGA/BMP-2 (Fig. 9d) alone. This result further determined that the combination of BMP-2 and HA had a synergistic effect in terms of osteogenic induction. It was interesting that the highest level of RUNX2 and OPN expression were found in the group treated with medium concentration of BMP-2, while highest level of OCN expression was found in the high concentration BMP-2 group. We speculated that medium concentration of BMP-2 could better induce the osteogenic differentiation of ADSCs during the early and middle stage of differentiation, while high concentration of BMP-2 was better for the late stage of differentiation.

Bone defects, caused by bone degenerative disorders, physical trauma and cancer, were in hare demand for bone grafts.[40] One of the major problems in bone repairing is lack of a sufficient of autograft and allograft bone. The implants made of biodegradable materials, which possess low immunogenicity and could be absorbed in the human body after several months to a year, offer an attractive approach for bone tissue engineering.[41] Another important advantage of the biodegradable implants in present study is that the cell-seeded implants can be delivered directly to the sites with a certain number of cells for tissue repairing, thus the cells seeded on the implants could be involved in tissue repair and accelerate tissue regeneration.[11] Multipotent mesenchymal stem cells have been widely used in tissue engineering for their potential to differentiate into multiple mesodermal tissue types including bone, cartilage, and adipose tissue.[42] Compared to bone marrow derived stem cells (BMSCs), ADSCs are ubiquitous, can be easily retrieved, require a less invasive procedure to harvest.[43] Moreover, it has been demonstrated that aging has no untoward effects on the regenerative properties of ADSCs and possesses the potential to induce bone regeneration.[44,45] It is believed that the biodegradable PLGA composites seeded with osteogenic differentiated ADSCs are of great value in bone repair.

On the other hand, active factors could make the biodegradable materials possess osteogenesis induction activity. The introduction of HA nanoparticles is important for the biodegradable PLGA composites when they were designed and fabricated specifically for bone tissue engineering. Firstly, the cell proliferation was increased by incorporation of HA due to its rough surface. Secondary, the levels of ALP activity and osteogenic gene expression of ADSCs were increased obviously by incorporation of HA, and the greatest effects were reached by the further combination of HA and BMP-2. BMP-2, a proven strong osteoinductive factor, is great in request in bone repair for stimulating the differentiation of osteoprogenitor cells into mature osteoblasts. The results of present study indicated that the PLGA composites incorporated with HA and surface-immobilized with BMP-2 might be optimal way for the improvement of osteogenic differentiation of ADSCs.

Furthermore, the Az-Gel was employed in this study for pre-modification of the biodegradable composites, which will provide an easy approach for surface immobilization of growth factors. Upon UV irradiation, azidophenyl groups of Az-Gel were photolyzed to generate highly reactive nitrenes that spontaneously formed covalent bonds with neighboring hydrocarbons on polymer surface. The surface-immobilized Az-Gel could efficiently improve the surface properties of PLGA composites, so that the ADSCs could adhere on the composites more easily and proliferate to sufficient number for osteogenic differentiation. Another advantage of Az-Gel is that the surface immobilization of BMP-2 *via* Az-Gel can not only reduce the amount of BMP-2, but also make the composites perform long-term osteoconductivity. However azidophenyl groups are regarded as foreign chemicals, the long-term effects of stability and toxicity during the retention of Az-Gel in the culture environment or organism should be taken into account when they were applied in tissue engineering. The clinically relevant indexes associated with Az-Gel such as mutagenicity, teratogenicity, carcinogenicity, reproductive toxicity, and genotoxicity will be determined in our future work.

Conclusions

In this study, we developed an effective surface modification method using photo-reactive gelatin *via* UV irradiation for the development of cell-adhesion and growth factor immobilization on the PLGA and PLGA/HA implants. BMP-2 was immobilized on the PLGA and PLGA/HA surfaces *via* Az-Gel. The cell adhesion and proliferation of ADSCs were greatly enhanced on the Az-Gel modified PLGA and PLGA/HA surfaces. Both the mixture of HA and the immobilization of BMP-2 performed the osteoinductive effects. Especially, the HA and BMP-2 showed the additive effect of promoting osteogenic differentiation of ADSCs. Moreover, the immobilization of BMP-2 *via* Az-Gel could not only decrease the growth factor consumption, but also perform long-term osteoinductive effect. Above all, the surface modification of PLGA implants shows a great potential for the development of biodegradable bone scaffolds and implants.

Acknowledgements

We gratefully acknowledge the financial support from the National Natural Science Foundation of China (No. 51273195, 51203152, 51473164, and 51403197), the Joint Research Project of CAS-JSPS (No. GJHZ1519), the International Science and Technology Cooperation Program of China (2014DFG52510), as well as the Major Project of Science and Technology of Jilin Province (20130201005GX).

References

1 Z. Ren, Y. Wang, S. Ma, S. Duan, X. Yang, P. Gao, X. Zhang and Q. Cai, *ACS Appl. Mater. Interfaces*, 2015, **7**, 19006–19015.
2 C. Q. Lyu, J. Y. Lu, C. H. Cao, D. Luo, Y. X. Fu, Y. S. He and D. R. Zou, *ACS Appl. Mater. Interfaces*, 2015, **7**, 20245–20254.
3 D. Li, H. Sun, L. Jiang, K. Zhang, W. Liu, Y. Zhu, J. Fangteng, C. Shi, L. Zhao, H. Sun and B. Yang, *ACS Appl. Mater. Interfaces*, 2014, **6**, 9402–9410.
4 D. Cheng, X. Cao, H. Gao and Y. Wang, *RSC Adv.*, 2013, **3**, 6871.
5 G. Chen, Y. Xia, X. Lu, X. Zhou, F. Zhang and N. Gu, *J. Biomed. Mater. Res., Part A*, 2013, **101**, 44–53.
6 P. F. Jiang, D. H. Yu, W. J. Zhang, Z. W. Mao and C. Y. Gao, *RSC Adv.*, 2015, **5**, 40924–40931.
7 D. Cheng, X. Cao, H. Gao, J. Hou, W. Li, L. Hao and Y. Wang, *RSC Adv.*, 2015, **5**, 17466–17473.
8 Y. Liu, H. Cui, X. Zhuang, P. Zhang, Y. Cui, X. Wang, Y. Wei and X. Chen, *Macromol. Biosci.*, 2013, **13**, 356–365.
9 N. H. Dormer, Y. Qiu, A. M. Lydick, N. D. Allen, N. Mohan, C. J. Berkland and M. S. Detamore, *Tissue Eng., Part A*, 2012, **18**, 757–767.
10 Y. Sun, Y. Deng, Z. Ye, S. Liang, Z. Tang and S. Wei, *Colloids Surf., B*, 2013, **111**, 107–116.
11 P. Zhang, H. Wu, H. Wu, Z. Lu, C. Deng, Z. Hong, X. Jing and X. Chen, *Biomacromolecules*, 2011, **12**, 2667–2680.
12 P. Zhang, Z. Hong, T. Yu, X. Chen and X. Jing, *Biomaterials*, 2009, **30**, 58–70.
13 T. Gao, N. Zhang, Z. Wang, Y. Wang, Y. Liu, Y. Ito and P. Zhang, *Macromol. Biosci.*, 2015, **15**, 1070–1080.
14 E. Ko, K. Yang, J. Shin and S. W. Cho, *Biomacromolecules*, 2013, **14**, 3202–3213.
15 H. Shen, X. Hu, F. Yang, J. Bei and S. Wang, *Acta Biomater.*, 2010, **6**, 455–465.
16 C. Y. Chien and W. B. Tsai, *ACS Appl. Mater. Interfaces*, 2013, **5**, 6975–6983.
17 T. Matsumoto, A. Yamada, R. Aizawa, D. Suzuki, M. Tsukasaki, W. Suzuki, M. Nakayama, K. Maki, M. Yamamoto, K. Baba and R. Kamijo, *PLoS One*, 2013, **8**, 10454–10461.
18 A. Neumann, A. Christel, C. Kasper and P. Behrens, *RSC Adv.*, 2013, **3**, 24222.
19 R. S. Nirmal and P. D. Nair, *Eur. Cells Mater.*, 2013, **26**, 234–251.
20 H. Wang, Q. Zou, O. C. Boerman, A. W. Nijhuis, J. A. Jansen, Y. Li and S. C. Leeuwenburgh, *J. Controlled Release*, 2013, **166**, 172–181.
21 J. C. Igwe, P. E. Mikael and S. P. Nukavarapu, *J. Tissue Eng. Regener. Med.*, 2014, **8**, 131–142.
22 M. H. Hettiaratchi, T. Miller, J. S. Temenoff, R. E. Guldberg and T. C. McDevitt, *Biomaterials*, 2014, **35**, 7228–7238.
23 Y. J. Lee, J. H. Lee, H. J. Cho, H. K. Kim, T. R. Yoon and H. Shin, *Biomaterials*, 2013, **34**, 5059–5069.
24 C. Shi, W. Chen, Y. Zhao, B. Chen, Z. Xiao, Z. Wei, X. Hou, J. Tang, Z. Wang and J. Dai, *Biomaterials*, 2011, **32**, 753–759.
25 H. Lu, N. Kawazoe, T. Kitajima, Y. Myoken, M. Tomita, A. Umezawa, G. Chen and Y. Ito, *Biomaterials*, 2012, **33**, 6140–6146.
26 B. Joddar, A. T. Guy, H. Kamiguchi and Y. Ito, *Biomaterials*, 2013, **34**, 9593–9601.
27 H. J. Cho, S. K. Perikamana, J. H. Lee, J. Lee, K. M. Lee, C. S. Shin and H. Shin, *ACS Appl. Mater. Interfaces*, 2014, **6**, 11225–11235.
28 W. Schuurman, P. A. Levett, M. W. Pot, P. R. van Weeren, W. J. A. Dhert, D. W. Hutmacher, F. P. W. Melchels, T. J. Klein and J. Malda, *Macromol. Biosci.*, 2013, **13**, 551–561.
29 J. W. Nichol, S. T. Koshy, H. Bae, C. M. Hwang, S. Yamanlar and A. Khademhosseini, *Biomaterials*, 2010, **31**, 5536–5544.
30 H. Makino, H. Hasuda and Y. Ito, *J. Biosci. Bioeng.*, 2004, **98**, 374–379.
31 H. Cui, Y. Wang, L. Cui, P. Zhang, X. Wang, Y. Wei and X. Chen, *Biomacromolecules*, 2014, **15**, 3146–3157.
32 G. J. Lai, K. T. Shalumon, S. H. Chen and J. P. Chen, *Carbohydr. Polym.*, 2014, **111**, 288–297.
33 Y. Cui, Y. Liu, Y. Cui, X. Jing, P. Zhang and X. Chen, *Acta Biomater.*, 2009, **5**, 2680–2692.
34 Y. Ito, H. Hasuda, T. Yamauchi, N. Komatsu and K. Ikebuchi, *Biomaterials*, 2004, **25**, 2293–2298.
35 K. Atluri, D. Seabold, L. Hong, S. Elangovan and A. K. Salem, *Mol. Pharmaceutics*, 2015, **12**, 3032–3042.
36 S. Kim, Y. Kang, C. A. Krueger, M. Sen, J. B. Holcomb, D. Chen, J. C. Wenke and Y. Yang, *Acta Biomater.*, 2012, **8**, 1768–1777.
37 S. Tada, T. Kitajima and Y. Ito, *Int. J. Mol. Sci.*, 2012, **13**, 6053–6072.
38 Q. Xie, Z. Wang, H. Zhou, Z. Yu, Y. Huang, H. Sun, X. Bi, Y. Wang, W. Shi, P. Gu and X. Fan, *Biomaterials*, 2016, **75**, 279–294.
39 B. Setzer, M. Bachle, M. C. Metzger and R. J. Kohal, *Biomaterials*, 2009, **30**, 979–990.
40 K. Chen, X. F. Lin, Q. Zhang, J. H. Ni, J. M. Li, J. Xiao, Y. Wang, Y. H. Ye, L. Chen, K. K. Jin and L. Chen, *Acta Biomater.*, 2015, **19**, 46–55.
41 P. Y. Zhou, X. S. Cheng, Y. Xia, P. F. Wang, K. D. Zou, S. G. Xu and J. Z. Du, *ACS Appl. Mater. Interfaces*, 2014, **6**, 20895–20903.
42 L. E. Kokai, K. Marra and J. P. Rubin, *Transl. Res.*, 2014, **163**, 399–408.
43 R. H. Lee, B. Kim, I. Choi, H. Kim, H. S. Choi, K. Suh, Y. C. Bae and J. S. Jung, *Cell. Physiol. Biochem.*, 2004, **14**, 311–324.
44 O. S. Beane, V. C. Fonseca, L. L. Cooper, G. Koren and E. M. Darling, *PLoS One*, 2014, **9**, e115963–e115963.
45 J. H. Lee, J. W. Rhie, D. Y. Oh and S. T. Ahn, *Biochem. Biophys. Res. Commun.*, 2008, **370**, 456–460.

